

TOWARD A MORE REALISTIC INTERFACE SHEAR STRENGTH EQUATION FOR COMPOSITE MEMBERS

Regina Waweru, PhD, Project Engineer, Huitt-Zollars, Dallas, TX; Former Doctoral Candidate, University of Texas at Arlington, Arlington, TX

Guillermo Palacios, M.Sc., Project Engineer, Jaster-Quintanilla, Dallas, TX; Former Master's student, University of Texas at Arlington, Arlington, TX

Shih-Ho Chao, PhD, PE, Associate Professor, University of Texas at Arlington, Arlington, TX

ABSTRACT

The shear resistance at the interface between the precast beam and the cast-in-place (CIP) slab is essential for the successful transfer of stresses. A good connection between the two components of the composite system can be achieved by artificially roughening the interface, providing a bonding agent, and/or using shear connectors or ties, mostly in the form of extended stirrups or hooks. The American Association of State and Highway Transportation (AASHTO) load-and-resistance factor design (LRFD) equation assumes that all reinforcement crossing the interface would be fully developed on both sides of the interface at the same time when the ultimate interface shear strength of the concrete is reached. This paper presents a multi-scale research-based investigation of push-off specimens and seven full-scale TxDOT beams to better understand the contribution of dowel action of the reinforcement on horizontal shear capacity, slip characteristics at horizontal shear failure, and the composite behavior at ultimate as a whole. No horizontal shear reinforcement was provided on two full-scale beams whereas the spacing of horizontal shear reinforcement varied on the box beams. The effect of the interface roughness was also investigated on full-scale beams by using self-compacting concrete (SCC) which results in a smoother surface finish. Three of the specimens were constructed with a reduced interface area to ensure a horizontal shear failure. A mid-scale beam and finite element analytical study were also conducted to further observe the influence of the net compressive force from live loads on horizontal shear strength. It was found that the current AASHTO LRFD specifications for interface shear strength in composite concrete beams do not necessarily reflect the actual behavior of the interface resistance mechanism by overestimating the interface shear contribution from dowel action of the reinforcement, and significantly underestimating the contribution from friction. AASHTO specifications only considers the permanent dead load when calculating the net compressive force normal to the interface (P_c) but fails to consider the contribution of the compression force generated by the live load on the interface which is the cause leading to ultimate failure.

Keywords: Friction, Prestressed Concrete, Composite Beam, Interface Shear Strength, Interface, Dowel Action.

INTRODUCTION

Sufficient shear resistance at the interface between the precast element and the cast-in-place (CIP) element is crucial in ensuring the successful transfer of stresses by preventing the relative slip between the two elements thus fostering composite action. Bonding is achieved by artificially roughening the surface, providing a bonding agent, and/or using shear connectors or ties, mostly in the form of extended stirrups or hooks. The horizontal shear at the interface is resisted by a combination of:

- (1) Resistance of the protrusions on the crack faces to shearing (i.e. cohesion and/or aggregate interlock) also referred to as the “cohesion factor” by AASHTO (2014)¹,
- (2) Friction between the crack faces, and
- (3) Dowel action of the reinforcement.

These components of horizontal shear resistance have been represented in the AASHTO equation for nominal shear resistance of the interface plane of composite concrete bridges by:

$$V_{ni} = cA_{cv} + \mu(A_{vf}f_y + P_c) \quad (1)$$

c = cohesion factor = 0.28 ksi for a CIP slab on clean concrete girder surface roughened to an amplitude of 0.25-in.;

μ = friction factor = 1.0 for a CIP slab on clean concrete girder surface roughened to an amplitude of 0.25-in.;

A_{cv} = interface area (in²);

P_c = net permanent compression force normal to the interface

However, the nominal shear resistance used for design shall not be greater than the lesser of $K_1f_cA_{cv}$ or K_2A_{cv} where K_1 and K_2 are 0.3 and 1.8 ksi respectively for normal weight concrete. $K_1f_cA_{cv}$ is a limit preventing shearing or crushing of aggregates whereas K_2A_{cv} is necessary due to lack of sufficient experimental data beyond the limit of K_2 .

The AASHTO equation is based on shear friction mechanism which states that as a rough interface slips, a wedging action develops forcing the crack to open in a direction perpendicular to the interface. As the crack opens, the reinforcement crossing the crack is engaged resulting in the generation of a clamping force ($A_{vf}f_y$). Thus the clamping force generated by horizontal shear reinforcements is passive in nature. Another source of the clamping force is compression force at the interface from loading conditions which are independent of the crack opening. Friction is assisted by the clamping force provided by the dead load of the CIP slab as well as that provided by the reinforcement bridging the interface. In order for the bars to develop their yield strength before pullout or debonding, the bars must

be sufficiently anchored on both sides of the interface. AASHTO limits the yield stress of interface reinforcement (f_y) to 60 ksi (AASHTO 2014 Section C5.8.4.1)¹ because previous research on pre-cracked specimens had determined that higher values of f_y overestimated the interface shear resistance.

The horizontal shear stress due to bending is equal in magnitude to the vertical shear stress and can be derived either based on the classical strength of materials approach or an alternative consideration of the shear force at strength limit state as given by AASHTO Section C5.8.4.2 (AASHTO, 2014)¹.

PAST RESEARCH ON SHEAR FRICTION

A number of researchers have investigated the shear friction mechanism and attempted to isolate the different components of shear resistance to determine their contribution.

Hanson² studied the composite action between concrete beam girders with CIP concrete slabs. He tested sixty-two push-off specimens and ten composite T-beams to investigate the horizontal shear transfer strength. The beams were designed to reach high horizontal shear at the interface of a load well below flexural failure. The beams were tested in two series: Series-I beams were loaded at two points, and Series-II beams were loaded at three points. From the results of the beam test, Hanson concluded that composite action was lost at the critical slip value of 0.005-in. He suggested that a maximum shearing stress for composite action to be 500 psi for a roughened bonded interface for concrete strength between 3000 psi and 5000 psi. If additional steel reinforcement crossing the interface is to be provided in excess of the required amount, an additional horizontal shear capacity of 175 psi may be added for each percent of stirrup reinforcement. Loov and Patnaik³ conducted an extensive study on the horizontal shear strength of composite concrete beams with roughened interface for a wide range of steel ratios. Sixteen composite beams with different geometries were tested. The major variables in their study were the clamping stress and the concrete strengths. The clamping stress was varied by adjusting the amount of steel crossing the interface and the width of the precast concrete girders. The interface was left as-cast with some aggregate protruding. The beams were simply supported and loaded with a point load at the center span. The beams were designed to be strong in vertical shear and flexure so that the first mode of failure would be horizontal shear. Their test showed that slip was insignificant up to a horizontal shear stress of 220 to 290 psi. It increased with stress up to a slip ranging from 0.01-in. to 0.03-in. They also observed that there was little difference between the shear stress at a slip of 0.2-in. and the shear stress at peak load. Their results showed that stirrups were not stressed until a horizontal shear stress was reached of about 220-290 psi and did not yield until a slip of 0.02-in. was reached. They concluded that elastic analysis using cracked transformed section properties is a valid assumption and a simple method for estimating the horizontal shear stresses in composite concrete beams at failure.

Although the two studies disagree on the slip required to yield the horizontal shear reinforcements, both show that slip has to occur first to engage the horizontal shear reinforcements. In order to develop the clamping force ($A_v f_y$), the crack must open sufficiently

to engage the bars. Crack width also greatly affects the cohesion component of shear friction because a larger crack width leads to reduced cohesion forces at the interface.

Seible and Latham⁴ conducted studies on the horizontal shear transfer behavior of overlaid reinforced concrete bridge decks combined with experimental results of the effects of interface preparations and dowels on horizontal load transfer. They stated that interface dowels are only beneficial in confining the crack after the fact.

As has been observed in past research and will be discussed in this study, the shear friction mechanism is complex in nature and is not accurately represented by the AASHTO equation. Push-off tests conducted by Waweru et al.⁵ indicated that shear resistance at the interface includes effects of dowel action, localized effects induced by the concrete in the vicinity of interface shear reinforcement at the interface, and the effects of aggregates, as well as concrete strength. Each push-off specimen measured 30×14×10 in. providing an interface area of 252 in² and was made of a precast segment and a CIP segment. The CIP part of the specimen was a 5-in. thick topping consistent with the CIP slab typically found on TxDOT box and slab beams.

MOTIVATIONS OF RESEARCH

AASHTO LRFD Bridge Design Specifications¹, section 5.8.4.1 requires that all reinforcement crossing the interface should be fully developed on both sides of the interface by embedment, hooks, or other method to develop the design yield stress. AASHTO Section 5.11.2.4 provides guidelines for determining the development length needed for standard hooks in tension. The equation provides results in an embedded length of 6.7-in. not possible in a 5-in. CIP slab. Typical embedded length of the interface shear reinforcement in current TxDOT prestressed slab beams and box beams is only about 2-in. (Figure 1). In addition, horizontal shear reinforcement does not qualify to be considered as “standard hooks” according to AASHTO, and there is no equation suitable for typical horizontal shear reinforcement. Since the shear friction action of the interface shear reinforcement relies on yielding of the bars (Item 3 of Eq. 1), a short embedded length inside the composite slab can lead to localized concrete fracture prior to yielding, thus providing insufficient clamping force. Push-off tests carried out by Waweru et al.⁵ showed that a 2-in. embedded length is insufficient to develop the yield strength and the bars were pulled out of the CIP slab well before that. The study also observed that for horizontal shear reinforcements embedded 4-in. into the CIP slab, pullout failure was suppressed. However, it was observed that the horizontal shear reinforcement did not yield at the onset of slip but rather yielded after the slip had occurred. The study proved that including horizontal shear reinforcement leads to an increase in horizontal shear strength of 50% or more regardless of the geometry and embedded length. This is believed to be due to the localized effects of the concrete engaged by the horizontal shear reinforcement that contributes to the overall shear strength. This study, therefore, further investigated the mechanism of dowel action and its contribution to horizontal shear resistance in full-scale beams. Of interest also is the effect of the high friction induced by the load. AASHTO specifications only consider the permanent dead load when calculating the net compressive force normal to the interface (P_c)

but in reality when ultimate failure occurs in a bridge it has to be due to a very high live load, which can contribute greatly to the normal force.

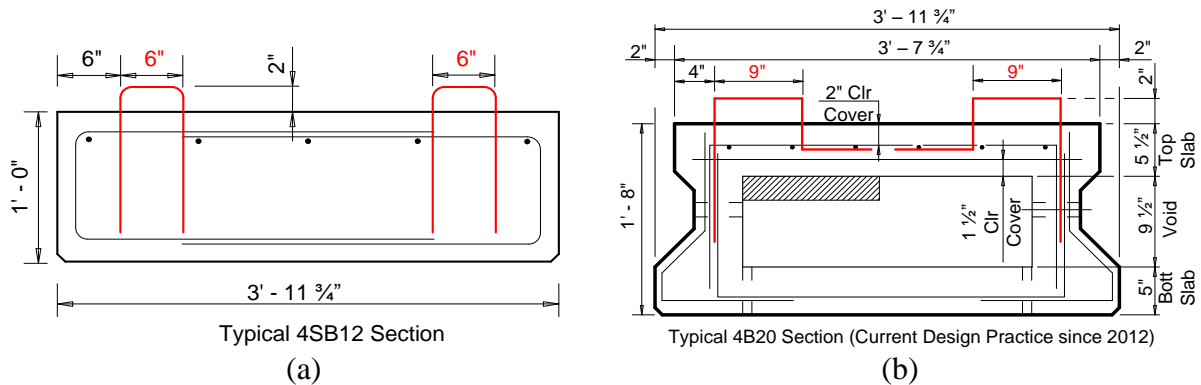


Fig. 1 Standard TxDOT (a) slab and (b) box beam details

An effective means to improve the horizontal shear resistance is to specify a rougher finish (i.e. amplitude of roughness greater than 0.25-in.) on top of the beam to improve horizontal shear capacity. Although AASHTO recommends a cohesion factor of 0.28 ksi for a surface roughened to an amplitude of 0.25-in., it does not address the fact that a smoother interface (Figure 2) may result from the use of self-consolidating concrete (SCC). Figure 2 shows the smooth surface of the SCC beam, even the workers used the same finish technique (wood float) that is used for conventional concrete. No other means were used by the workers to increase the roughness. Consequently, there is no cohesion and friction factor suggested in the case where SCC is used. Although an experimental study carried out by Saemann and Washa⁶ postulated that increasing the surface roughness leads to an increase in the horizontal shear strength, Walraven and Reinhardt⁷ showed that an increase in surface roughness resulted in an increase in crack width. Therefore, testing SCC beams would provide valuable information to determine the effect of a much smoother interface on the horizontal shear resistance.



Fig. 2 Surface finish on SCC slab beams (approximately corresponding to CSP4; does not meet 0.25-in. amplitude)

EXPERIMENTAL PROGRAM

TEST SPECIMENS

Geometry of Full-scale Specimens

Four full-scale composite TxDOT slab beams (type 4SB12) and three TxDOT box beams (type 4B20) were fabricated. The precast beams with a 5-in. composite deck were fabricated and instrumented at a precast plant in Houston and then delivered to UT Arlington for testing. The slab beams measured $360 \times 47.75 \times 12$ -in. (length \times width \times height) whereas the box beams measured $360 \times 47.75 \times 20$ -in. One of the box beams (4B20#1) and slab beams (4SB12#1) was designed using the current reinforcement detail according to TxDOT specifications to represent a typical beam used in practice (Figure 1). The same detailing was maintained for the other three slab beams (4SB12#2, 4SB12#3, and 4SB12#4) with the addition of flexural reinforcement in order to achieve a shear demand higher than the strongest TxDOT box beams and slab beams typically used in practice. The flexural reinforcements were placed in the most convenient spacing in order to avoid congestion with the strands and facilitate concrete placement (Figure 3). Horizontal shear reinforcements were excluded from 4SB12#2 slab beam as they had been determined from component test (Waweru et al.⁵) to have minimal contribution towards horizontal shear resistance.

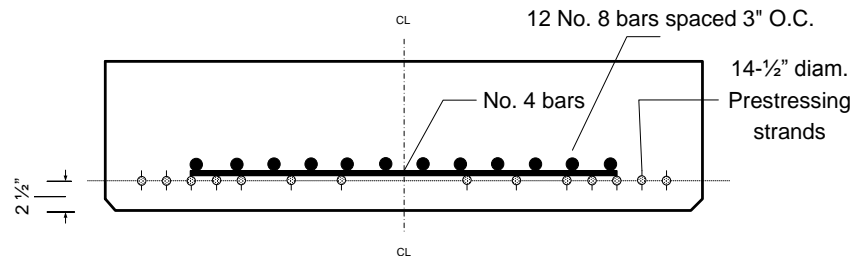


Fig. 3 Slab beam without shear reinforcement

In order to force a horizontal shear failure, the interface surface was reduced in the last two slab beams with conventional concrete (4SB12#3) used in one and SCC in the other (4SB12#4). The size of interface area needed to ensure a horizontal shear failure was calculated based on both the elastic method (VQ/Ib_v) and the simplified elastic method (V/b_vd). Three different contact widths (10-in., 12-in., and 14-in.) were used for the calculations and the resulting horizontal shear stress compared to the demand horizontal shear stress. A reduction of the contact area to 12-in. width in slab beams was found to be adequate to cause horizontal shear failure. Therefore the contact area was reduced from a 47.75-in. width to a 12-in. width in the slab beam. The area was reduced by the use of foam tape placed on the surface of the beams thereby intentionally reducing the interface area.

The second box beam (4B20#2) had similar detailing as the first box beam with the inclusion of flexural reinforcement to simulate the flexural strengths of the strongest TxDOT slab and box beam typically used in practice. No horizontal shear reinforcements were provided on the box beam as it was determined from component tests to have minimal contribution to the peak shear strength (Figure 4). The interface area was reduced in the last

box beam (4B20#3) in order to force horizontal shear failure to occur. Four No. 8 longitudinal mild steel rebars were added to increase the shear demand (Figure 5). Horizontal shear reinforcement was provided at a spacing of 24-in., the maximum spacing allowed by AASHTO¹. A wood float finish was used to roughen the interface. Similar to slab beams, the size of interface area needed to ensure a horizontal shear failure was calculated based on both the elastic method (VQ/Ib_v) and the simplified elastic method (V/b_vd). Three different contact widths (10-in., 12-in. and 14-in.) were used for the calculations and the resulting horizontal shear stress compared to the demand horizontal shear stress. A reduction of the contact area to 14-in. width (using foam tape) in the box beam was found to be sufficient to lead to horizontal shear failure. Therefore, the contact area was reduced from 43.75-in. width to 14-in. width.

Two common finishes used in Texas plants at the interface were investigated; a rake finish and a wood float finish. A 5-in. thick CIP slab was later cast on the precast beams to form a composite beam section. The beams were designed to ensure tension-controlled behavior and to exclude premature vertical shear failure even with the additional longitudinal reinforcement. Strain gauges were mounted on the flexural reinforcements to measure strain on the rebars during the test and on the horizontal shear reinforcement to provide useful information to check the calculations. PGSuper⁸ was used to design the box and the slab beams.

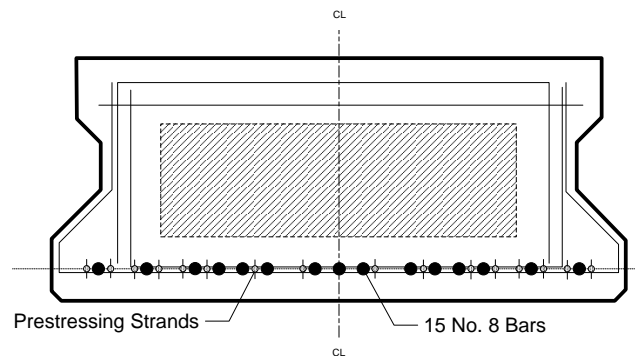


Fig. 4 Box beam without shear reinforcement

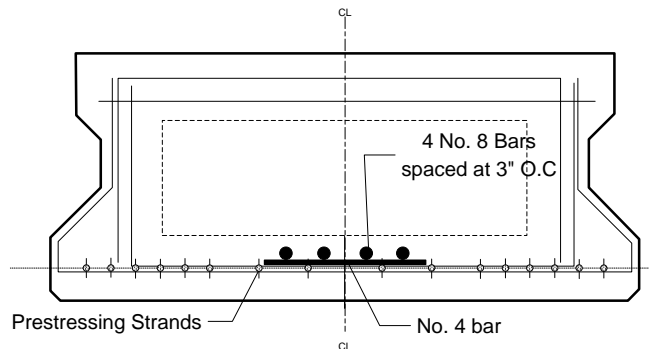


Fig. 5 Beam 4B20#3 section showing tension reinforcements

The prestressing strands were stressed at a jacking force of 31 kips per strand. Strain gauges were installed on the longitudinal bars and on stirrups. Concrete cylinders were made and the 28-day compressive strength of the precast beam was found to be 11 ksi while that of the CIP slab was found to be 10 ksi. A rake finish was provided on specimen 4SB12#1,

4SB12#2, 4B20#1 and 4B20#2 whereas a wood float finish was provided on 4SB12#3, 4SB12#4 and 4B20#3. Strain gauges were installed on the horizontal shear reinforcement prior to casting of the CIP slab (Figure 6). The foam tape was then placed on the surface of the beams with reduced interface thereby intentionally reducing the interface area (Figure 7). The interface area of the slab beam was reduced from 47.75-in. to 12-in., and the interface area for the box beam was reduced from 43.75-in. to 14-in. The foam tape was placed in two layers to guarantee that no tear will occur during casting of the CIP slab. The CIP part of the specimens was cast with concrete Class “S” as shown in Figure 8.



Fig. 6 Strain gauges installation on horizontal shear reinforcements



Fig. 7 Interface (a) without and (b) with foam tape on interface



Fig. 8 Finished CIP slab

TEST SETUPS AND PROCEDURES

Three-point loading was selected for this test because of the uniform shear force along the beam, which generates the interface shear stress along the entire beam. The beam was monotonically loaded at the center (Figure 9) except for 4B20#3 and 4B20#4 beams which were loaded 7 ft from the support (Figure 10) to increase the shear demand. The test set-up for the full-scale beams was composed of a reaction frame with a hydraulic cylinder attached to apply the load. Two W12 \times 72 wide flange sections were used as the loading beam (stacked one on top of the other) so as to apply the load uniformly along the width of the composite beam. A load cell was placed between the hydraulic cylinder and the loading beam to record the load. The specimen was instrumented with three linear varying differential transformers (LVDTs) placed at the interface to measure the relative slip between the precast and CIP parts during testing. Two LVDTs were placed under the midpoint of the beam to measure the displacement during loading whereas one LVDT was placed at each support to measure displacements. To reduce any load eccentricities, the actual position of the loading beam and load cell were marked on the specimen before testing. The load was then applied on the beam at different loading intervals up to failure.

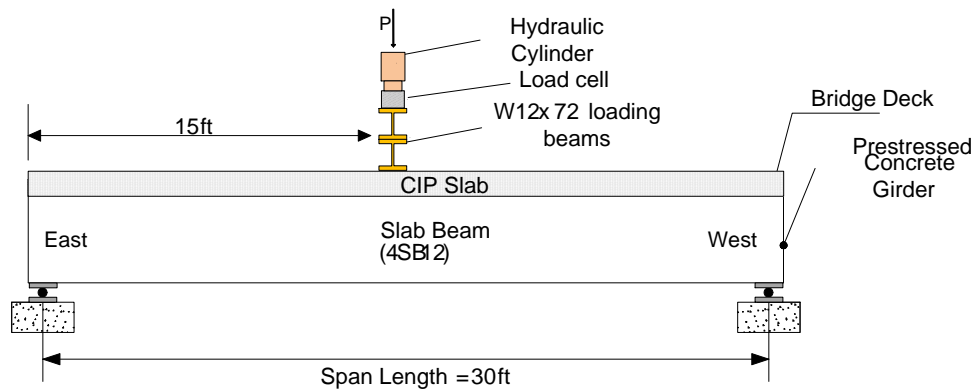


Fig. 9 Schematic view of the slab beam test set-up (north-side view)

The box beam 4B20#3 was loaded 7 ft. from the support to increase the shear demand. Once one side of the box beam was tested (Figure 10 (a)), the beam was flipped and the other side of the box beam was tested at 7 ft. from the support (Figure 10 (b)). The specimens were instrumented with two LVDTs placed on both the CIP and precast parts to measure the slip during testing. One LVDT was placed under the mid-span of the beams to measure the displacement during loading whereas one LVDT each was placed at the supports to check for any settlement occurring at the supports.

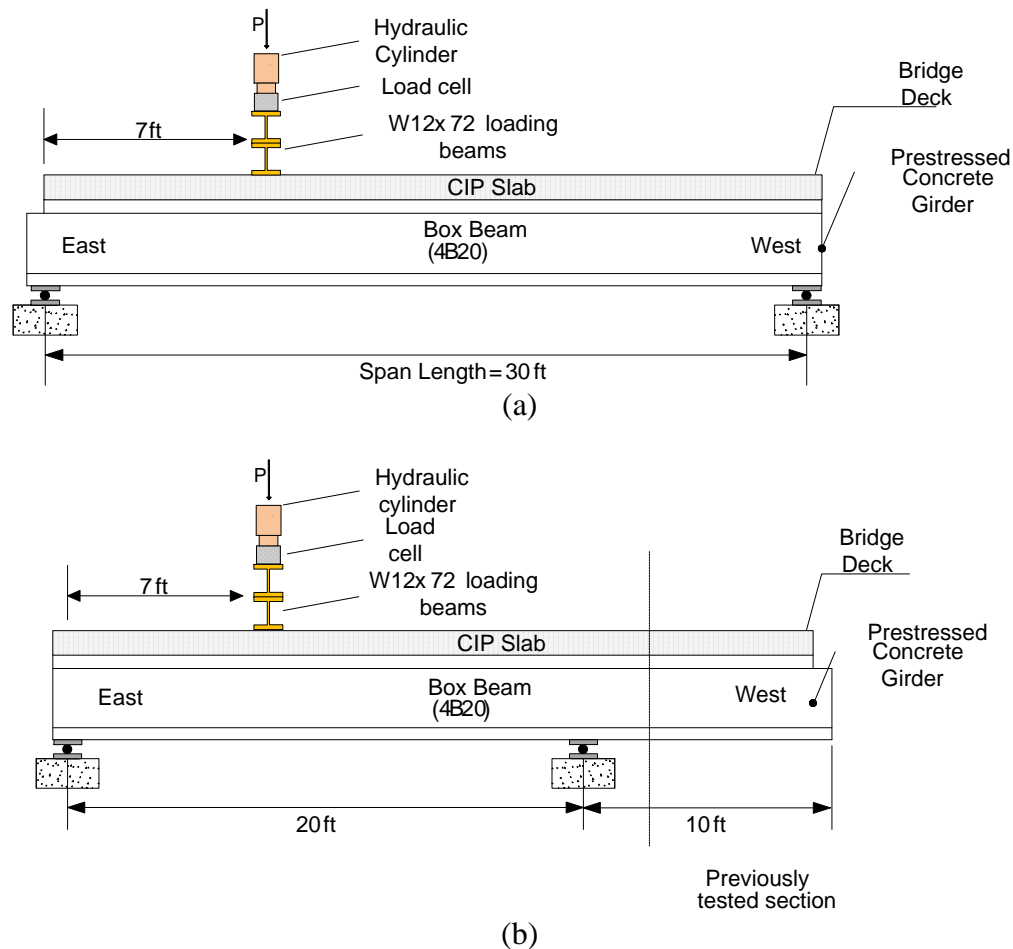


Fig. 10 Schematic view of (a) (4B20#3) and (b) (4B20#4) box beam test set-up (north-side view)

OVERALL BEHAVIOR OF FULL-SCALE BEAMS

Beam 4SB12#1 (current TxDOT slab beam details) was loaded monotonically in intervals of 5-10 kips interval until failure. The beam failed in flexure at a peak load of 102 kips corresponding to a displacement of 7-in. with crushing of concrete under the loading point. No cracks and slips at the interface were observed. No significant strain was measured from the horizontal shear reinforcement, thus indicating a very minor contribution from the horizontal shear reinforcement. Beam 4SB12#2 (slab beam without horizontal shear reinforcement) also failed at flexure at a load of 197 kips despite lack of horizontal shear reinforcement and intentionally increased shear demand. Upon further loading, an explosive failure occurred with a decrease in load of more than 100 kips and the formation of a horizontal crack 2-in. below the interface. The interface remained intact without any cracks forming across it. Although some hairline cracks propagated along the interface at failure on the south-face side, it did not extend further and was not observed on the north-face side of the beam. Beam 4SB12#3 (slab beam with reduced area) showed an increase in strains in the horizontal shear reinforcements at 150 kips. Slip between the CIP slab and precast beam occurred at a load of 156 kips. At 170 kips and a mid-span displacement of 3.6-in., a slip of 0.015-in. was

recorded at the east-end of the beam with an increase in the crack width at the same end. With the development of shear cracks at the beam ends, the strains in the horizontal shear reinforcement continued to increase. At a load of 175 kips, yielding was observed in the horizontal shear reinforcement located at the beam ends as shown in the load-slip plot (Figure 11). The beam failed in flexure at a load of 181 kips and a displacement of 6.65-in. Crushing of concrete occurred near the loading point and the flexural cracks significantly widened to more than 0.24-in.. A separation between the CIP slab and the precast beam was also observed with a slip of 0.15-in. being recorded (Figure 12). From strain gauge information, it was clear that almost all the horizontal shear reinforcement had yielded at this point.

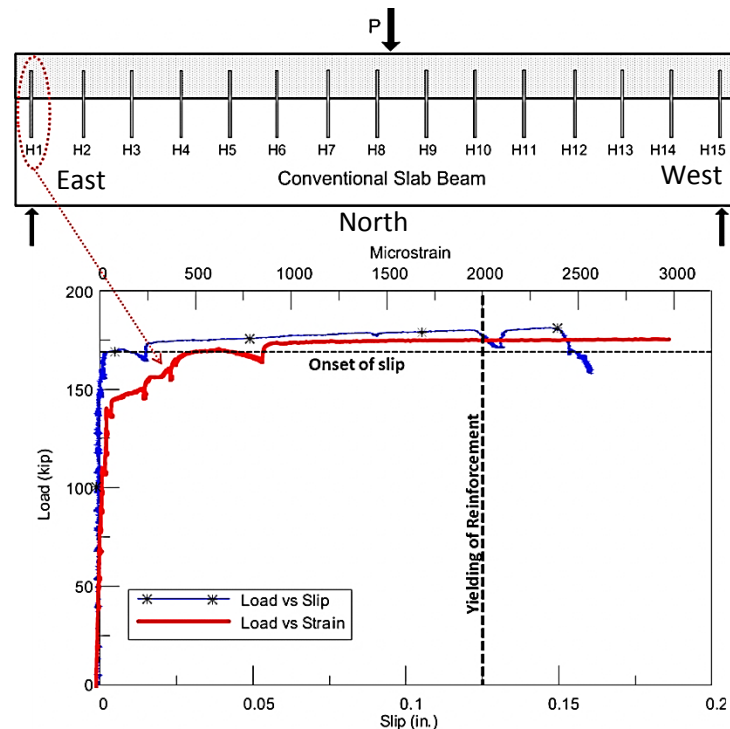


Fig. 11 Beam 4SB12#3 load versus slip and strain plot



Fig. 12 Beam 4SB12#3 at failure showing separation of the interface

Beam 4SB12#4 (SCC slab beam with reduced area) experienced slip of 0.0024-in. at a load of 130 kips. Strains in the horizontal shear reinforcement began increasing gradually. The flexural cracks continued to propagate towards the loading point with new flexural cracks forming along the length of the beam. Slip gradually increased as the load was increased. At a load of 160 kips, a slip of 0.015-in. was recorded. Cracks at the interface became noticeably larger at both ends of the beam. Horizontal shear reinforcement near the support yielded at a load of 173 kips and a slip of 0.04-in. The beam failed by flexure at a load of 192 kips with crushing of the concrete under the loading point. A slip of 0.12-in. was recorded. Crushing of concrete was, however, observed on both the CIP slab and the precast beam (Figure 13). The wide crack opening at the interface and the concrete crushing at both the slab and the beam indicated that composite action was partly lost.

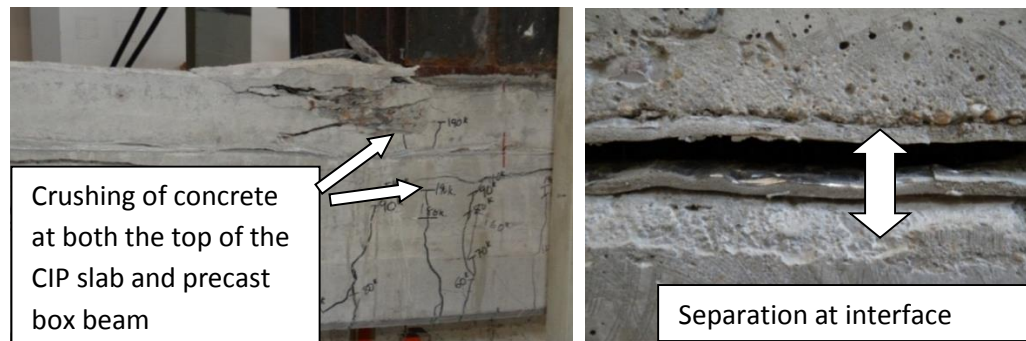


Fig. 13 Beam 4SB12#4 at failure with separation at the interface

Box beam 4B20#1 (current TxDOT standard) failed in flexure due to concrete crushing in the compression zone within the CIP slab. No cracking was observed within the interface of the prestressed beam and the CIP slab, and no strains were recorded on the horizontal shear reinforcement. Similarly, beam 4B20#2 (box beam without horizontal shear reinforcement) failed at flexure at a load of 400 kips. With increase in load, the concrete crushed and the cracking propagated into the interface leading to a sudden horizontal shear failure. However, the horizontal shear crack did not propagate through the entire length of the beam. Therefore no slip was recorded by the LVDTs at the ends.

Beam 4B20#3 was loaded at 7 ft. away from one end of the beam. Load was applied at intervals of 10 kips until the first flexural crack was observed at a load of 160 kips. At 190 kips, more flexural cracks formed along the beam length. Very small strain was recorded from the horizontal shear reinforcement at this point. At a load of 247 kips, a cracking noise was heard and the load dropped to 225 kips as evident from the load vs slip plot in Figure 15. Interface slip was recorded to be 0.024-in. at that instance. Strains in the horizontal shear reinforcement also began to increase. Cracks on the CIP slab began to appear at a load of 250 kips. These cracks were observed not to have originated from the flexural cracks on the precast beam. Interface cracks widened markedly with a slip of 0.08 in. being recorded. Yielding of horizontal shear reinforcement close to the end of the beam occurred at a load of 263 kips with a slip of 0.09-in. The crack at the interface widened to 0.06-in.. With an increase in load to 270 kips, the crack at the interface widened to 0.05-in. Flexural failure occurred at 287 kips with a deflection of 5.4-in. Crushing of concrete was observed on both the CIP slab and the

precast beam. A slip of 0.60-in. was recorded at the end of the test. Severe concrete fracture was observed on the east end of the beam as seen in Figure 16 near the interface. A large separation along the interface was also observed (Figure 17) as well as a noticeable slip at the beam end.



Fig. 14 Beam 4B20#3 (a) top view and (b) side elevation of test set-up

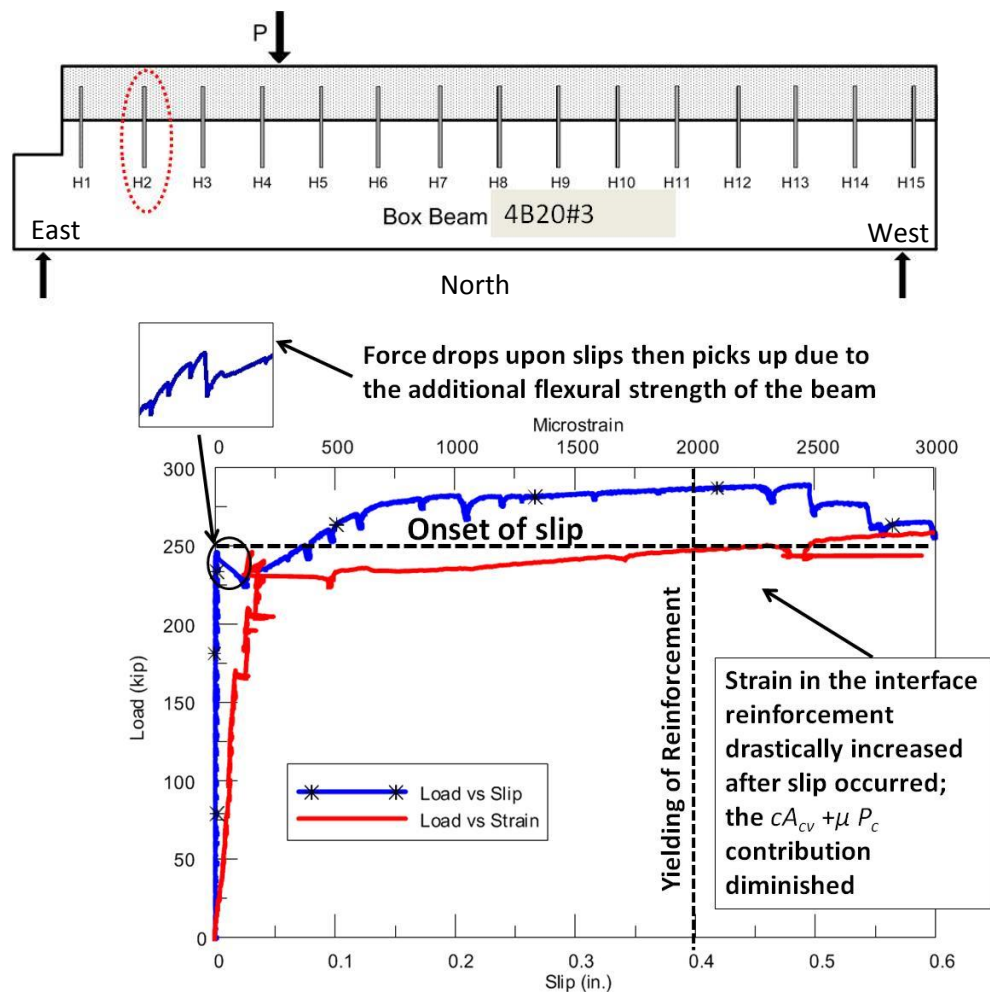


Fig. 15 Load-slip and load-strain plot for box beam 4B20#3



Fig. 16 Beam 4B20#3 at failure with concrete fracture at the east-end



Fig. 17 Separation between the CIP slab and precast beam on beam 4B20#3 at failure

It is important to note the majority of horizontal shear strength before the onset of slip can be attributed to the cohesion and friction of the concrete. Figure 17 shows how a separation at the interface looks; such a separation can trigger a load drop after the onset of slip. The separation indicates the diminished contribution of cohesion and friction, and the engagement of the horizontal shear reinforcement—signified by an increase in strain up to yielding of the horizontal shear reinforcement (as slip is reached at 0.4-in.) as shown in the load-strain plot. This may suggest that the AASHTO (2014) horizontal shear equation does not accurately predict the true behavior of composite beams. Indeed, Eq. 1 assumes that the peak strengths of cohesion, friction, and dowel (yielding) occur simultaneously.

The box beam 4B20#4 was then flipped and the beam loaded 7 ft. from the other side of the box beam. Cracks were observed within the CIP slab at a load of 240 kips with a hairline crack forming at the interface between the CIP slab and the block-out area. An interface slip of 0.008-in. was recorded at a load of 250 kips with a widening of the interface crack being observed. There were, however, small strains recorded in the horizontal shear reinforcements. At a load of 320 kips, the interface crack widened with interface slip increasing to 0.028-in. The beam failed by flexure at a load of 388 kips due to crushing of the concrete at the CIP slab and precast beam underneath the loading point. An interface slip of 0.25-in. was recorded at failure.

Figure 18 shows the load-slip and load-strain plots for the box beam 4B20#4. It is important to note that the strain in the horizontal shear reinforcement did increase until close to the onset of slip, after which the strain continues to increase up to yielding. The strain in the horizontal shear reinforcement at the onset of slip is observed to be $500 \mu\epsilon$ which then rapidly increases to yielding ($2000 \mu\epsilon$) with increase in load after slip (0.2-in.) occurs. This observation is consistent with that observed on 4B20#3.

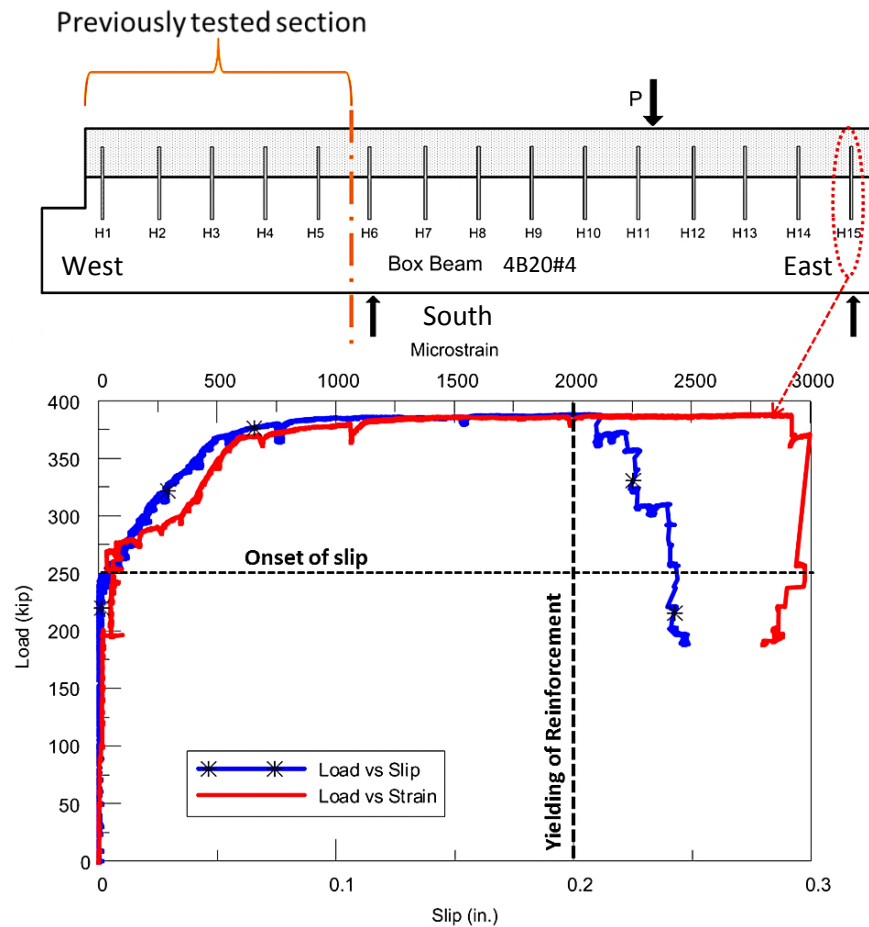


Fig. 18 Load-slip and load-strain plot for box beam 4B20#4

Table 1. Full-scale beam test results

Specimen	Failure Load (kips)	Load at the onset of slip (kips)	Failure Mode	Strain ϵ_{su} on horizontal shear reinforcement at onset of slip ($\mu\epsilon$)
4SB12 #1	101	-	Flexure	100
4SB12 #2	195	-	Flexure	-
4B20 #1	193	-	Flexure	250
4B20 #2	407	-	Flexure*	-
4SB12#3-conventional	181	156	Horizontal Shear/ Flexure**	340
4SB12#4 -SCC	192	130	Horizontal Shear/ Flexure**	560
4B20#3-no block-out	284	247	Horizontal Shear/ Flexure**	200
4B20#4 –block-out	388	250	Horizontal Shear/ Flexure**	500

* Horizontal shear failure was a secondary failure after flexural failure had occurred.

** Interface slip/separation occurred but did not propagate throughout the beam due to the high friction near the loading point. The beams showed very large flexural deformation and significant yielding in the longitudinal reinforcement.

VALIDATION OF RESULTS USING FINITE ELEMENT ANALYSIS

From the full-scale testing it is observed that the separation between CIP slab and the precast beam could not occur near the loading region. Obviously this is because of the normal loading which induced high friction in the vicinity of that region. In actual bridges, should the ultimate failure occur, a very high live loading needs to be applied, which could also considerably increase the friction, which would ultimately prevent the beams from losing their composite behavior. However, current AASHTO provisions only consider the contribution of permanent dead load.

In the full-scale beams, we did not use extensive instrumentation to monitor the presence of the local high compressive stresses. To further investigate this behavior, a smaller scale T-beam (Figure 19) was prepared which had more intensive instrumentations such as internal concrete strain gauges. A T-beam was used to purposely reduce the interface area so it would fail along the interface. A finite element model using LUSAS program was also created to investigate the distribution of the applied load along the specimens. The FE model was used to check the compressive stresses at the interface along the composite beam. The beam consisted of a precast beam measuring 96×10×10-in. (length×width×height) and a CIP slab measuring 96×24×5-in. (length×width×height). A 3-dimensional (3D) analysis of the beam was conducted (Figure 19). For simplicity, the reinforcements were not incorporated into the model. The concrete to concrete interface was connected to one another assuming a perfect

bond. The model was created in two sections to allow for the formation of the interface. The beam was modeled as simply supported with a pin connection on one end and a roller connection on the other. The supports acted through the centerline of the supported area. A point load was applied at a distance 48-in. from the support.

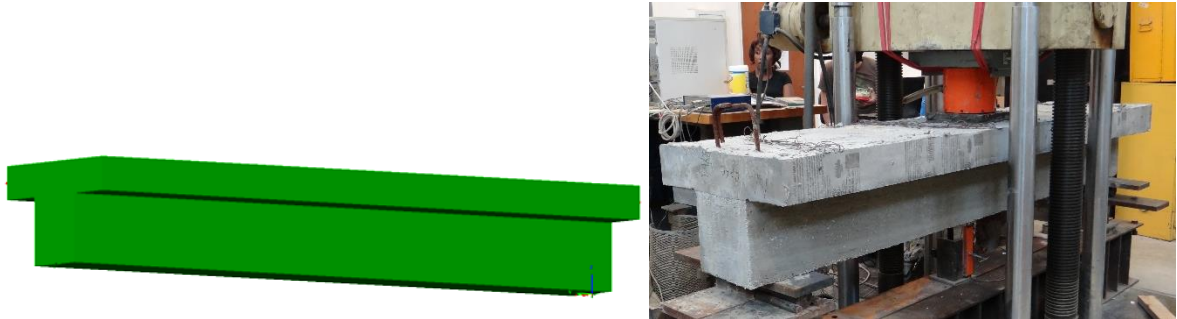


Fig. 19 T-beam 3D model and actual testing

FE ANALYSIS SUMMARY AND TESTING RESULTS

The compression stresses along the entire beam were analyzed as shown in Figure 20. The interface stresses were also analyzed and the compressive stresses along the beam plot. It is clear that the compressive stresses are highest near the loading point and gradually reduce (almost linearly) towards the support. These results support our hypothesis that the high compressive stresses at the loading point keep the interface crack from opening at that point; hence, lower strains were recorded in the horizontal shear reinforcements. Note that the resulting friction can be much higher than just using the permanent dead load. Experimental results in Figure 20 also show that while local slips could occur, no slips could happen in the vicinity of the loading region, which maintain the composite behavior of the entire beam.

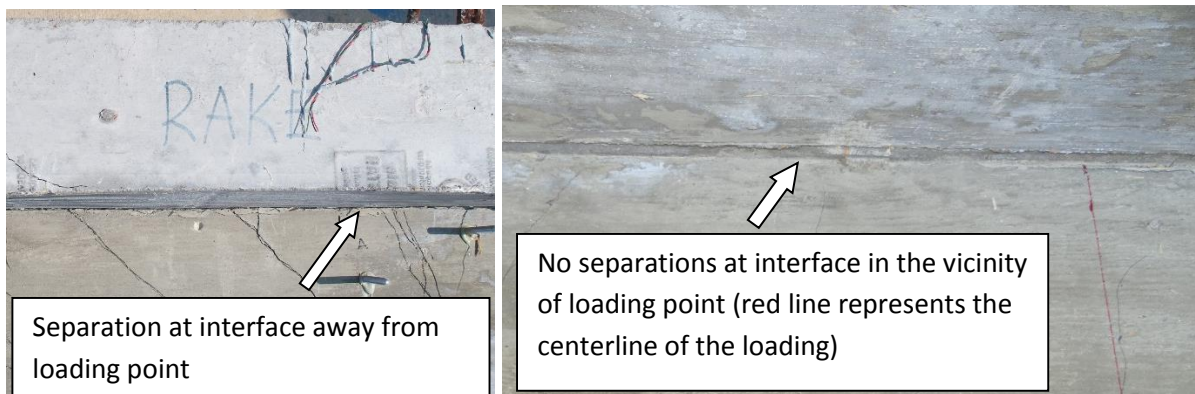
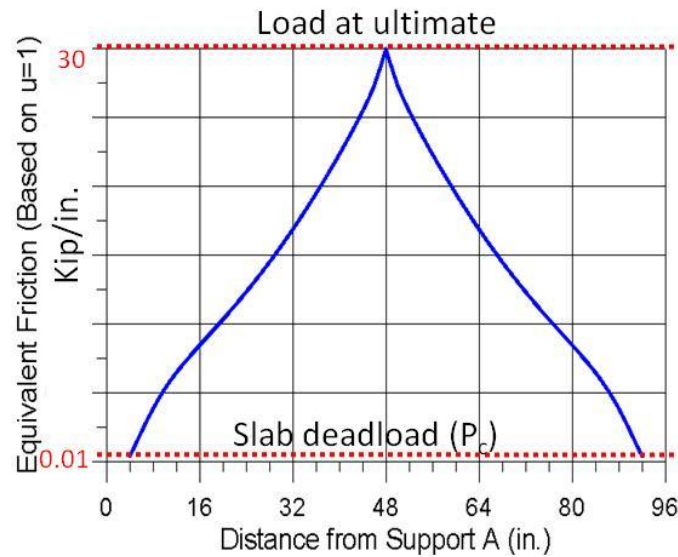


Fig. 20 Compressive stress vs distance from support plot

DISCUSSION OF RESULTS

Tests results revealed that horizontal shear failure will not occur in TxDOT box and slab beams with current design practice as was observed on beams 4SB12#1 and 4B20#1. Throughout the testing of box and slab beams with horizontal shear reinforcement, no significant strain was measured according to the strain gauge data of the horizontal shear reinforcement because the beams always failed by flexure first. The horizontal shear strength from concrete alone was sufficient to resist the shear stress at ultimate flexural failure.

Interface areas of all beams were purposely reduced in the last three beams by foam tapes to decrease the horizontal resistance and force the beams to fail along the interface before flexural failure. This was done to obtain the actual horizontal shear strength and to verify the data from the component tests. The reduced areas in the slab and box beams were reduced by 75% and 66%, respectively. The test revealed that slab beams made with SCC experienced slip

at a lower load (130 kips) as compared to the slab beam having conventional concrete (156 kips). The slip was noted to be equal on both ends of the beam for the SCC slab beam whereas the slip on the conventional concrete occurred only on the east half of the beam. At ultimate failure, the slip at a deflection of 6.8-in. was found to be higher in conventional concrete compared to SCC. Although the SCC slab beam experienced interface slip at a smaller load than the conventional concrete slab beam, it actually reached a slightly higher peak load compared to the conventional concrete. This shows that it still maintained the composite action. This is evident also from strain gauge information whereby the horizontal shear reinforcement yielded at a load of 190 kips compared to the conventional concrete whereby most horizontal shear reinforcement yielded at a load of 160 kips.

Slip was observed to occur in both beams before yielding in the horizontal shear reinforcement. It is noted from Figure 21 that in the SCC beam, the separation was much smaller than that in the beam made of conventional concrete. This can be attributed to smaller asperities in SCC compared to conventional concrete. As the aggregate/crack surface rides or slides on each other during slip, smaller asperities will lead to less crack width at interface thus leading to SCC retaining more composite action and thus lower slip at failure and a 6% higher failure load.

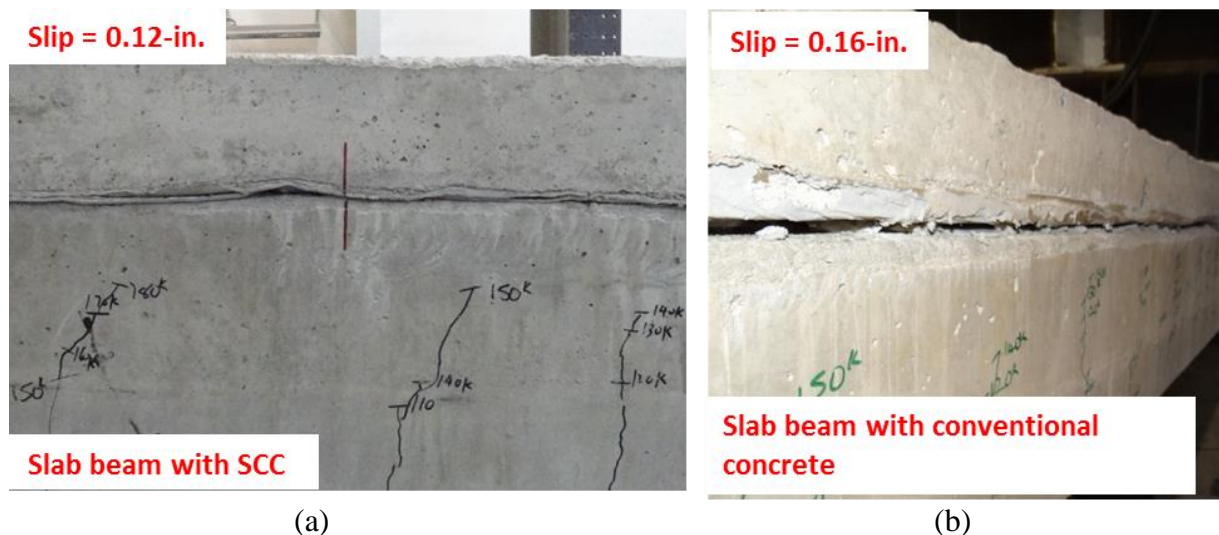


Fig. 21 Slab beam (a) 4SB12#3 and (b) 4SB12#4 slip at failure

Similar results were observed for the box beam with reduced interface area. The beam experienced slip before yielding of the horizontal shear reinforcement. Both tests resulted in flexural failure with crushing being observed on both the CIP slab and the precast beam. This is an indication that composite action had been partially lost.

Comparing the horizontal shear capacity (using elastic beam theory) at the onset of slip to the AASHTO estimated results, it is found that AASHTO equation results in a horizontal

shear stress that is 27% higher than that recorded in the conventional beam and 56% higher than that recorded in the SCC beam.

Effect of High Compression Force Due To Loading

It was also noted that due to a high compression force at the loading point, there was increased confinement and resistance to slip due to increased friction. This is also evident on the beams at failure as no slip or interface crack was observed at or near the loading point. This ultimately prevented the slab from separating from the beam, thereby maintaining certain composite action. Indeed, the ultimate strengths of 4SB12#2, 4SB12#3, and 4SB12#4 are nearly the same even with separation occurred in 4SB12#3 and 4SB12#4. Strain gauge profile plots support these findings as shown in Figure 22. The strain gauge profile shows that while the strains increase rapidly after slip on horizontal shear reinforcements away from the loading point (especially the ones at the ends), horizontal shear reinforcements at or near the loading point experience much smaller strains from slip to failure of the beam.

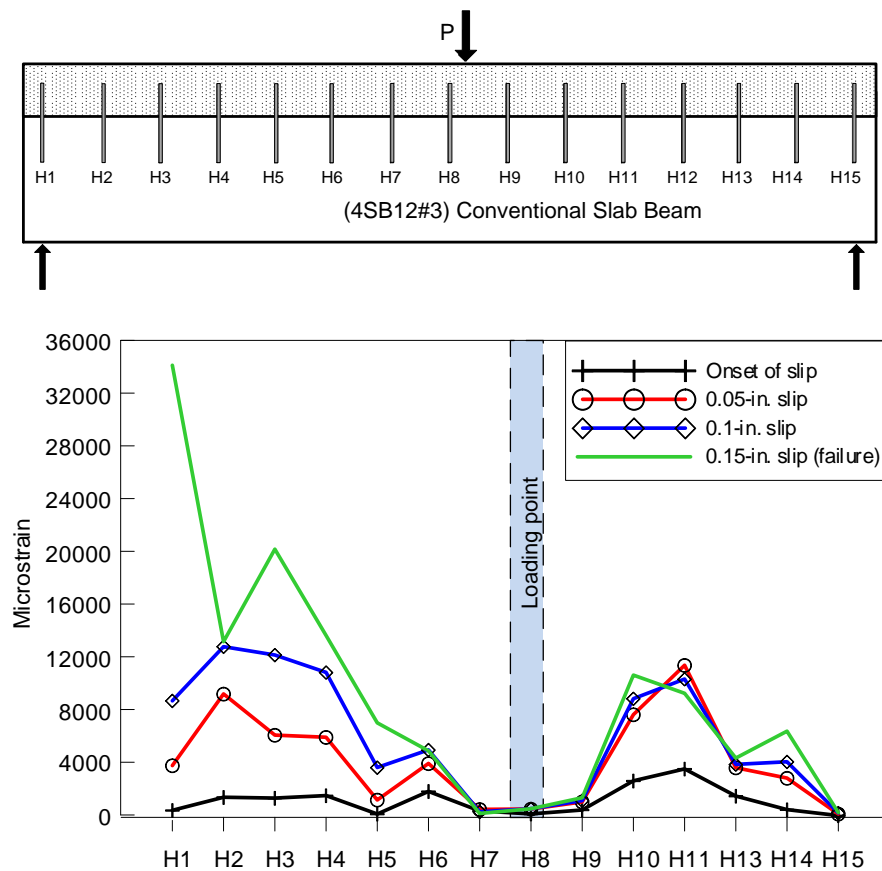


Fig. 22 Strain profile along beam length

FE analysis also supports this finding as shown earlier whereby the compressive stresses at the interface are seen to be high and decrease almost linearly towards the supports. In actual bridges, the increased friction could cover a wider range of the span because the

AASHTO HL-93 loading usually considers a combination of distributed live load (design lane load) and the design truck or design tandem.

The compressive force from the live load on the bridge girder could provide additional friction resistance at the interface. AASHTO equation considers the deck weight and other superimposed loads as contributing to the P_c factor but fail to consider that live loads are the dominant loads that lead to failure of a beam either in flexure, shear or horizontal shear. The P_c (permanent net compressive force) force from the AASHTO equation could be modified to consider part of the live load which will lead to an increase in the friction force (μP_c) and consequently to an increase in the horizontal shear capacity.

CONCLUSIONS AND RECOMMENDATIONS

1. The use of SCC does reduce slightly the horizontal shear strength by 17% due to reduction in cohesion and friction. However SCC has less separation at the interface; thus, the specimen using SCC maintains a higher degree of composite action. Test results from this project indicate that using SCC can provide sufficient strength for the slab beams.
2. Although the push-off tests show that interface reinforcement with a 2-in. embedded length could not be fully developed (Waweru et al., 2014)⁵, the full-scale tests (with reduced interface area) indicate that the actual boundary conditions in the composite beams could provide abundant confinement to develop the reinforcement. Also, the compressive force resulting from loading on the full-scale beams prevents bars from being pulled out.
3. At ultimate horizontal shear capacity, the horizontal shear force is mainly resisted by the cohesion/aggregate interlock and friction from the concrete with minor contribution from the interface shear reinforcement. The interface shear reinforcement became engaged only after slip/separation occurred at the interface (also indicated by Seible and Latham⁹, Hofbeck et al.¹⁰, and Kent et al.¹¹).
4. Current AASHTO equation overestimates the contribution of the interface shear reinforcement at ultimate horizontal shear capacity by assuming that the reinforcement has yielded when ultimate horizontal shear capacity is reached. Tests revealed that the strength of horizontal shear reinforcement at horizontal shear failure was 30% of the expected contribution from the bars.
5. Based on findings from this study, in order to reflect the actual behavior of horizontal resistance, the interface shear resistance contribution from the reinforcement can be reduced, while the force (μP_c) can be increased by considering not only the permanent load but partial live load. The increase or decrease in the aforementioned components of horizontal shear resistance is currently under analytical and experimental investigation.

ACKNOWLEDGEMENTS

We gratefully acknowledge the financial support from Texas Department of Transportation (TxDOT) under project No. 0-6718 and would like to especially thank Project Director, Darrin Jensen for his supervision and support of this research, as well as constructive comments given by former Project Director, Amy Smith.

REFERENCES

- 1) AASHTO, "LRFD Bridge Design Specifications," 7th edition, American Association of State Highway and Transportation Officials (AASHTO), Washington, D.C., 2014.
- 2) Hanson, N. W., "Precast-Prestressed Concrete Bridges: (2) Horizontal Shear Connections," PCA Journal, 2(2): 38-58, 1960.
- 3) Loov, R. E., and Patnaik, A. K., "Horizontal Shear Strength of Composite Concrete Beams with a Rough Interface," PCI Journal, 39(1): 48-69, 1994.
- 4) Seible, F., and Latham, C. T., "Horizontal Load Transfer in Structural Concrete Bridge Deck Overlays," Journal of Structural Engineering, ASCE, V. 116, No. 10, pp. 2691 – 2710, 1990.
- 5) Waweru, R., Palacios, G., and Chao, S.-H., "Horizontal Shear Strength of Full-Scale Composite Box And Slab Bridge Beams Having Horizontal Shear Reinforcement with Limited Development Length," 2014 PCI Convention and National Bridge Conference, September 6-9, 2014, Washington, D. C.
- 6) Saemann, J. C., and Washa, G. W., "Horizontal Shear Connections between Precast Beams and Cast-In-Place Slabs," ACI Journal, 61(11): 1383-1409, 1964.
- 7) Walraven, J. C., and Reinhardt, H. W., "Theory and Experiments on the Mechanical Behaviour of Cracks in Plain and Reinforced Concrete Subject to Shear Loading," Heron, V. 26, No. 1A, 68 pp., 1981.
- 8) Texas Department of Transportation, PGSuper Design Guide, 2013.
- 9) Seible, F., and Latham, C. T., "Horizontal Load Transfer in Structural Concrete Bridge Deck Overlays," Journal of Structural Engineering, ASCE, V. 116, No. 10, pp. 2691 – 2710, 1990.
- 10) Hofbeck, J. A., Ibrahim, I. O., and Mattock, A. H., "Shear Transfer in Reinforced Concrete," ACI Journal, 66(13): 119-128, 1969.
- 11) Kent, A. H., Gabriel, Z., Bahram, S., "Toward an Improved Understanding of Shear-Friction Behavior," ACI Journal, 109(6): 835-844, 2012.